

Extra Dimensions, Dark Energy, and the Gravitational Inverse-Square Law

Liam J. Furniss
Department of Physics and Astronomy
Humboldt State University
One Harpst Street
Arcata, CA 95521-8299. USA

Faculty Advisor: Dr. C.D. Hoyle, Jr.

Abstract

Although gravity was the first fundamental force of nature to be described mathematically by Isaac Newton over 300 years ago, it remains at the forefront of current physics and astronomy research. Einstein's refined theory of gravity, General Relativity, has passed all experimental tests to date, but it is fundamentally inconsistent with the Standard Model of quantum mechanics that successfully describes all three other known fundamental interactions. In an effort to perform a "unification" that provides a consistent framework incorporating both theories, String Theory suggests that our universe may contain more than the three observed spatial dimensions. These "extra dimensions" may alter the gravitational inverse-square law at small but measurable (sub-millimeter) distance scales.¹ Many other unification scenarios predict new short-range forces mediated by exotic subatomic particles.² In addition, recent observations of the cosmic distance scale acceleration,³ attributed to an unknown phenomenon called Dark Energy, lead to the belief that gravity could be fundamentally different from how it is now characterized. Due to its extreme weakness relative to the other fundamental forces of nature, a short-range gravitational experiment requires an extremely high-sensitivity instrument such as a precision torsion pendulum. At Humboldt State University, we are establishing a new laboratory to probe the gravitational inverse-square law at unprecedented levels in the sub-millimeter regime with a novel parallel-plate torsion pendulum. This apparatus will improve upon previous results⁴ and provide world-leading tests of gravitational theory over unexplored distance scales. This paper addresses the motivation, experimental design, and preliminary results from the laboratory.

Keywords: Gravity, Extra Dimensions, Inverse-square Law, Dark Energy

1. Introduction and Motivation

Theoretical speculations that seek to solve the largest remaining puzzles in physics have, in recent years, suggested that gravity may behave in a non-standard way at extremely short distances. Some of these speculations are motivated by string theory, while others are attempts to explain unexpected cosmological observations, often referred to as the "Dark Energy" or "vacuum energy" problem. One of the most definitive of the string theory proposals predicts that gravity gets stronger at distances comparable to the size of proposed "rolled-up" extra dimensions.¹ Attempts to explain dark energy, on the other hand, have shown that data would be consistent with a theory that predicts gravity to "turn off" at distances less than about 0.1mm.⁵ Finally, unobserved particles such as the dilaton and radion may produce new short-range forces that could be observed in tests of gravity.²

These speculations offer experimentalists an opportunity to search for new physics by testing the behavior of short-range gravity. By looking for unexpected deviations from the "normal," Newtonian gravitational interaction at extremely short ranges, the parameter space for new physics can be explored and constrained.

New gravitational behavior is generally modeled using a Yukawa addition to the classical Newtonian potential. For point masses m_1 and m_2 separated by distance r , the potential becomes

$$V(r) = -\frac{Gm_1m_2}{r} \left(1 + \alpha e^{-r/\lambda}\right), \quad (1)$$

where G is the gravitational constant, α is a dimensionless scaling factor corresponding to the strength of any deviation relative to Newtonian gravity, and λ is the characteristic length scale of the deviation. Previous experiments utilizing various types of torsion pendulums have eliminated large portions of the Yukawa potential parameter space.^{4,6} Our method improves on previous experiments with a novel parallel-plate pendulum design and attractor drive system that is largely insensitive to classical Newtonian gravitational torques, while highly sensitive to short-range effects. Figure 1 shows the progress previous experiments have made in constraining the Yukawa potential α - λ parameter space.

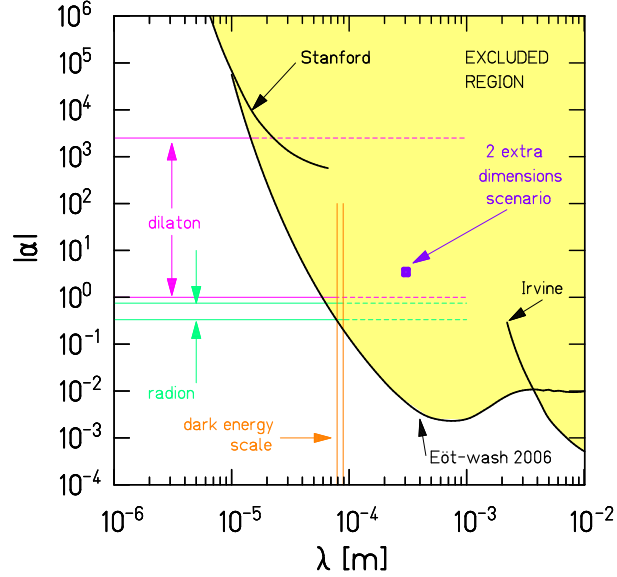


Figure 1. Existing Yukawa potential parameter constraints.

Figure 1 shows current short-range experimental constraints in the α - λ Yukawa parameter space. The shaded region is excluded at the 95% confidence level. Results from previous experiments are shown by the curves labeled Stanford,⁷ Eöt-Wash,⁶ and Irvine.⁸ For a more detailed discussion of the various constraints and theoretical predictions, see Figure 6 of Reference 6.

2. Experimental Technique

To achieve the sensitivity required to test for deviations, it is necessary to decouple the test masses as much as possible from normal, Newtonian gravitation. The standard approach is to use a torsion pendulum, which naturally separates the experiment from terrestrial gravity. Our approach extends on this with a stepped pendulum and a comparatively large attractor plate arranged in a parallel-plate configuration as shown in Figure 2. The attractor-pendulum separation is modulated at drive frequency ω . The parallel-plate design is inherently more sensitive to short range effects than previous “vertical” configurations because it utilizes the full force vector instead of a single component to produce torque on the pendulum. At sufficiently small separation distances, this setup is insensitive to the normal, inverse-square law interaction, while being highly sensitive to anomalous short-range behavior.

By choosing a drive frequency sufficiently different from the torsion pendulum's resonant frequency, ω_0 , we decouple the signal from many external disturbances that will excite resonant motion, and avoid being sensitive to the pendulum's natural mode of oscillation. The modulated twist of the pendulum will be measured optically by reflecting laser light from the pendulum's polished surface and recording the beam deflection with an optical autocollimator. The attractor plate's relatively large size compared to the pendulum size and separation distance ensures a small signal from any normal, inverse-square torque, as the attractor's Newtonian gravitational field will be nearly uniform throughout the pendulum.

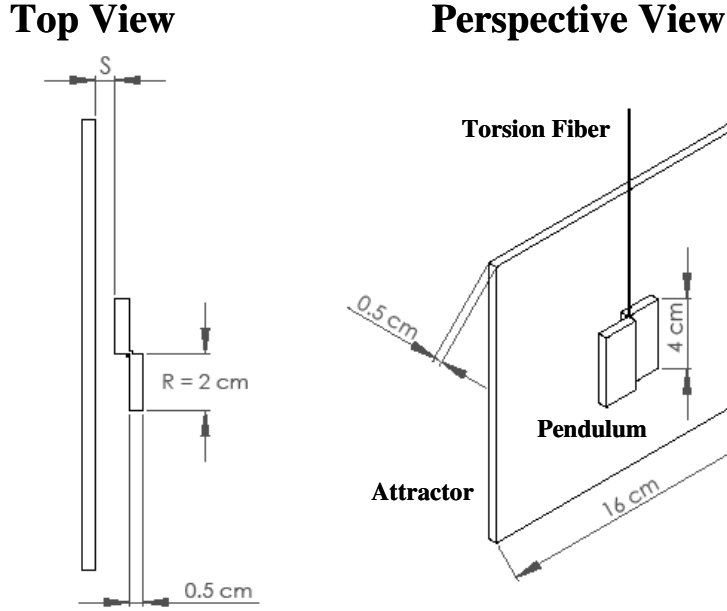


Figure 2: Pendulum and attractor geometry.

Figure 2 shows the geometry of the pendulum and attractor plate. The pendulum's steps result in different short-range torques applied to each side, which in turn results in a twist, harmonic at a frequency equal to the chosen drive frequency for the attractor plate modulation. The pendulum is made from aluminum and the attractor is copper.

The new "force" that might be seen by this method will not drop-off as the usual inverse of distance squared; it will drop-off much more quickly with increasing separation. In particular, for λ much smaller than the characteristic size of the pendulum and attractor, the Yukawa torque may be approximated as

$$N_Y \approx \pi \alpha G \rho_p \rho_a R A \lambda^2 e^{-s/\lambda} , \quad (2)$$

where ρ_p and ρ_a are the mass densities of the pendulum and attractor, respectively, s is the separation between the pendulum and attractor, A is the area of one pendulum "step," and R is the width of the step (see Figure 2). The Newtonian background torque is computed analytically, assuming the plates are rectangular.⁹ We chose aluminum for the pendulum material so that a thin torsion fiber may be used. This thin fiber provides an increased sensitivity that more than compensates for any increase in Yukawa signal with the use of a high-density material. A copper attractor is easily machined, while having a relatively high density. More exotic, high-density materials may be used in future iterations of the experiment.

For the analysis in this paper, we assume a pendulum geometry shown in Figure 2. Figure 3 compares the expected gravitational torque on the pendulum with a hypothetical Yukawa torque as a function of pendulum-attractor separation distance, s . For this plot, the Yukawa parameters are assumed to be $\alpha = 1$ and $\lambda = 100 \mu\text{m}$. The attractor and pendulum are assumed to reach a minimum separation of $s_{\min} = 100 \mu\text{m}$, and the attractor plate has a peak-to-peak modulation of 1 mm.

In addition to the pendulum and attractor, other key components of the experiment are the torsion fiber itself and the optical angle readout, or autocollimator. The torsion fiber is a $20 \mu\text{m}$ diameter tungsten wire of length $\sim 0.5 \text{ m}$ and load capacity is approximately 100 g. The torsion constant κ determines the sensitivity of the apparatus to a large extent. A smaller value of κ indicates a weaker restoring force and a larger twist angle for a given applied torque. For this setup, $\kappa = 0.06 \text{ erg/rad}$.

In order to measure the tiny torques evident in Figure 3, a very precise angle readout system is required. The autocollimator reflects a 670 nm laser beam from a polished surface of the pendulum, returning the beam via a beam splitter to a position-sensitive photodiode (see Figure 4). The photodiode signals are recorded and converted to twist angle in LabVIEW, our primary data acquisition system. Temperature fluctuations, vacuum chamber pressure, and other environmental data are recorded as well.

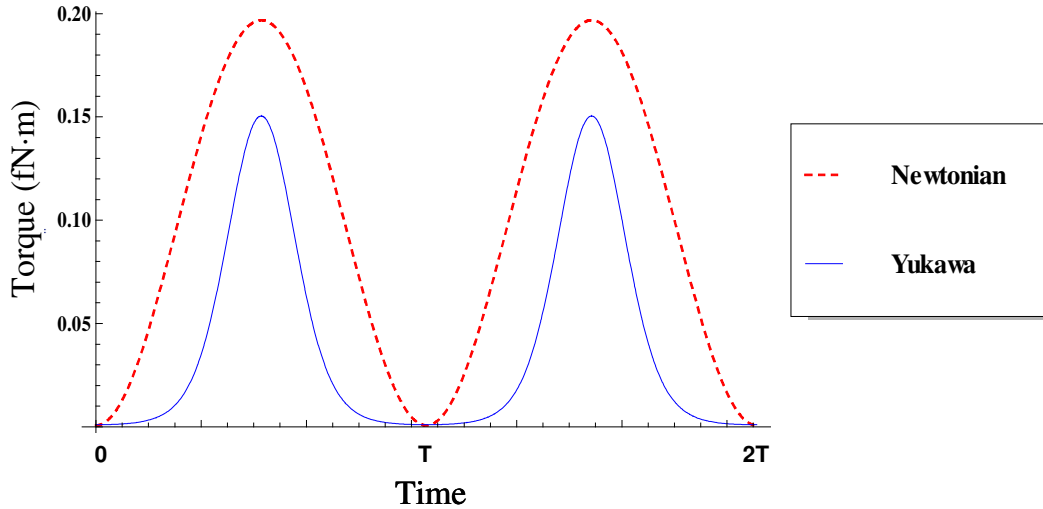


Figure 3: Sample Newtonian and Yukawa torques on the pendulum.

Figure 3 shows calculated Newtonian and Yukawa torques on the pendulum as a function of time for two complete attractor modulation cycles with oscillation period, T . We assume a peak to peak modulation amplitude of 1 mm and minimum separation of $100 \mu\text{m}$. We see that while the Newtonian torque is larger, the Yukawa interaction with $\alpha = 1$ and $\lambda = 100 \mu\text{m}$ would be clearly evident, as it would add measurably to the Newtonian signal.

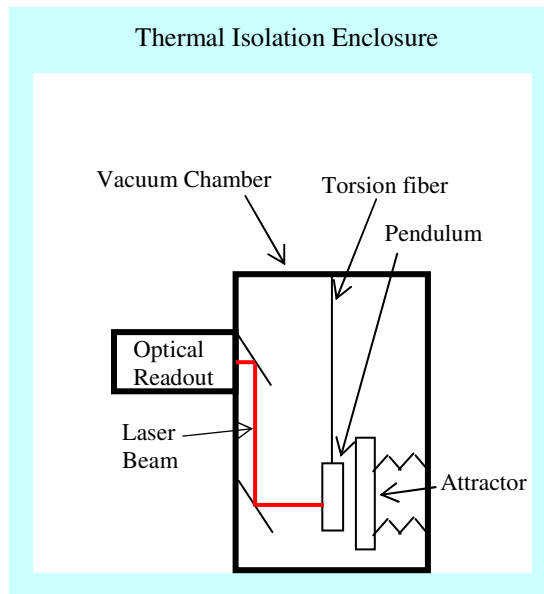


Figure 4. Schematic of the experimental setup.

3. Sensitivity

To probe for new interactions, our system must be sensitive to torques on the order of 10^{-18} Nm . This will require resolution in the optical system on the order of nanoradians. The sensitivity of the experiment will be determined by the uncertainty in the measurement of the torque on the pendulum produced by the attractor plate, which is limited by a number of fundamental issues. The two most important sources of statistical noise arise from the dynamics of the torsion pendulum itself and the optical angle readout.

The angular deflection of a torsion pendulum subject to both viscous and internal damping obeys the relationship

$$N = I\ddot{\theta} + b\dot{\theta} + \kappa\left(1 + \frac{i}{Q}\right)\theta, \quad (3)$$

where N is the applied torque, I is the moment of inertia of the pendulum, θ is the angular deflection, b is the viscous damping parameter, and Q is the quality factor associated with the internal losses in the torsion fiber material ($Q \sim 4000$ for tungsten). For our purposes, we may assume negligible velocity damping, $b \approx 0$, because our pendulum resides in a high-vacuum environment (see section 5.1 and Figure 4).

The first major noise source arises in the optical readout and the associated electronics, δN_{ro} . This torque noise increases with frequency, ω , as the torsion pendulum's resonant motion tends to hide driving signals with frequencies much greater than its resonant frequency:

$$\delta N_{ro}(\omega) = (\delta\theta_{ro})\kappa\sqrt{\left(1 - \frac{\omega^2}{\omega_0^2}\right)^2 + \left(\frac{1}{Q}\right)^2}. \quad (4)$$

In equation (4), $\delta\theta_{ro} = 10^{-7} \text{ rad}/\sqrt{\text{Hz}}$ is angular noise of the optical angle readout (similar to other such readout systems⁴). Second, thermal noise in the torsion fiber contributes to error in a way that is also dependent on frequency, but unlike optical readout noise, it decreases with increasing drive frequency. Thermal noise in the torsion fiber contributes to torque noise by the relationship:

$$\delta N_{th}(\omega) = \sqrt{\frac{4k_B T \kappa}{\omega Q}}, \quad (5)$$

Where k_B is Boltzmann's constant and T is the ambient temperature in Kelvin. Combining these uncertainties in quadrature determines the "sweet spot" for the attractor plate drive frequency, where the torque noise is minimum:

$$\delta N(\omega) = \sqrt{(\delta N_{ro}(\omega))^2 + (\delta N_{th}(\omega))^2}. \quad (6)$$

The individual noise sources, as well as the total torque noise, are plotted as a function of frequency in Figure 5. If limited by only these statistical sources, and given a 30-day integration time, our torque sensitivity will be $5 \times 10^{-19} \text{ Nm}$, well within the desired range.

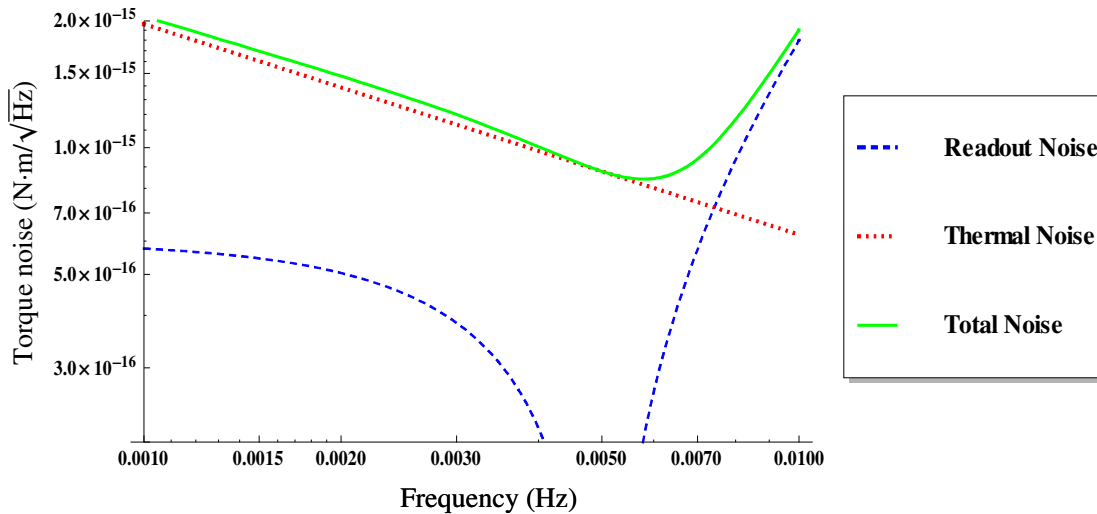


Figure 5. Torque noise as a function of frequency.

Figure 5 shows the thermal noise in the torsion fiber as well as the readout noise as a function of frequency. The total noise quadrature sum is also shown. The plot shows that the optimal attractor plate drive frequency will be 5.7 mHz, corresponding to an oscillation period of approximately 175 seconds. The corresponding noise level at this frequency is $8 \times 10^{-16} \text{ Nm}/\sqrt{\text{Hz}}$.

4. Expected Results

Assuming we reach the level of torque sensitivity determined in the preceding section, we set the minimum measurable Yukawa torque to be $N_Y = 5 \times 10^{-19} \text{ Nm}$ and use equation (2) to produce an expected sensitivity in the α - λ parameter space as shown Figure 6. We see that this sensitivity exceeds that of previous experimental efforts by up to two orders of magnitude.

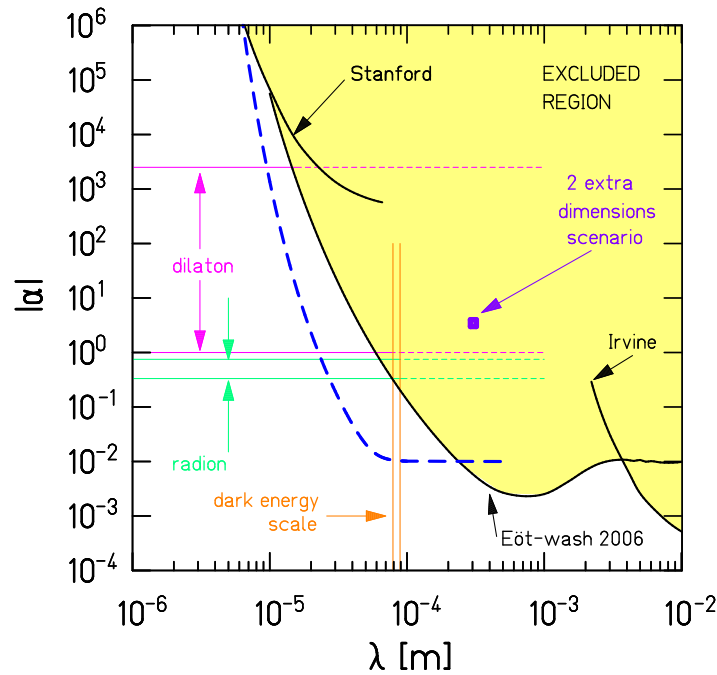


Figure 6. Expected Yukawa sensitivity.

The dashed line in Figure 6 shows the predicted sensitivity of the apparatus. Note that for some values of λ , we achieve a factor of approximately 100 improvement over previous efforts. We assume a conservative minimum resolution in α of 1% to account for measurement uncertainty of the pendulum and attractor geometries and mass distributions.

5. Limitations and Possible Systematic Errors

In order to reduce possible sources of systematic errors due to environmental effects, we insulate the apparatus as much as possible from its surroundings. Possible sources of systematic error include temperature fluctuations, laboratory floor tilt, vibrations, and electromagnetic interactions which are inherently much stronger than gravity.

5.1 vacuum chamber

In order to avoid viscous damping noise and direct thermal coupling to the pendulum, the entire pendulum and attractor are contained in a high-vacuum chamber. This chamber was custom built by Atlas Technologies for purposes of this research. It consists of an aluminum body with ten removable flanges allowing input for such devices as the optical system and pendulum suspension while still maintaining vacuum. The roughing pump is a

Varian SH-110 Dry-Scroll Pump, while the high vacuum is maintained by a Varian LP-70 turbomolecular pump. Measurements of the vacuum have shown pressures as low as 10^{-6} Torr, well below the viscous regime for this pendulum.

5.2 thermal isolation enclosure

To isolate the experiment from local temperature fluctuations we have constructed an insulated enclosure for the apparatus. To further ensure temperature stability, the chamber has a programmable thermoelectric temperature controller (TE Technology, Model TC-24-25) with control stability and resolution of ± 0.1 K. Temperature can be controlled from -20° C to $+100^{\circ}$ C using a PID feedback loop from the readout of a MP-2379 thermistor. Figure 7 shows measured thermal fluctuations inside and outside the enclosure.

5.3 fiber suspension system

The torsion fiber itself consists of two sections. Suspended at the junction of the sections, approximately 3 cm from the upper fiber attachment point, is a disk that resides in a magnetic field gradient. This magnetic “damper” uses eddy current effects to suppress the simple pendulum “swing” and the vertical “bounce” modes of oscillation. The cylindrical nature of the disk ensures that it does not damp torsional motion.

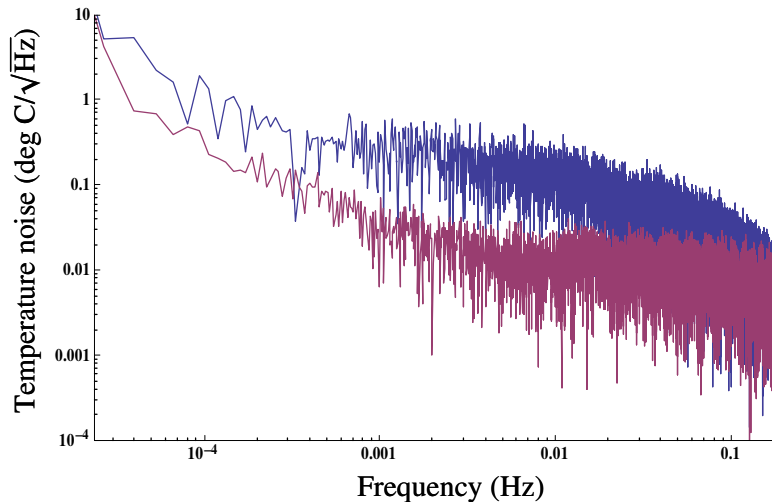


Figure 7. Thermal fluctuation suppression of the isolation enclosure.

Figure 7 shows the effectiveness of the thermal isolation enclosure. Over the entire frequency range, the fluctuations in temperature are reduced markedly inside the enclosure (lower data) versus outside (upper data).

5.4 tilt sensor

A custom-built tilt sensor will be installed to measure the time-varying tilt of the apparatus. Knowledge of the tilt is important because of the well-documented tilt-twist effect in torsion fibers.⁴ This sensor is a dish filled with a dielectric fluid. Either side of the dish will act as a capacitor along with the liquid in the middle. As level of the liquid on either side changes, so will the capacitance. Because the device is gravity based, the surface of the liquid will always be perpendicular to local vertical. The tilt angle precision that can be obtained by such a system is one arc-second or smaller. This system is not affected by variations in the temperature and by its nature cancels out the noise of unassociated shocks or vibrations.

5.5 electrostatic shield

As we are working in a vacuum with metal plates, the Casimir effect or local patch charges may cause varying forces at the drive frequency and contribute large systematic error to our measurements. To combat these effects,

we insert a metal membrane between the pendulum and the attractor plate. The membrane is made of stretched Beryllium Copper and will completely electrically shield the pendulum and attractor.

6. Conclusion and Outlook

We are well on our way to obtaining world-leading measurements of gravity at short distances. Such results will be useful for characterizing theoretical scenarios that suggest gravity may behave in a fundamentally different way at sub-millimeter scales. Such predictions arise in string theory, particle physics, and cosmology (in the framework of dark energy models). With a novel parallel-plate torsion pendulum design, we performed the calculations described in this paper and predict our sensitivity will exceed existing experimental efforts by up to a factor of 100.

We have constructed our initial apparatus including vacuum chamber, thermal isolation enclosure, and data acquisition system. The optical angle readout and pendulum will be finished shortly. We expect to produce preliminary constraints on deviations from the inverse-square law by the end of this year.

7. Acknowledgements

We are thankful for financial support from Research Corporation (Cottrell College Science Award CC6839), the Humboldt State University College of Natural Resources and Sciences (CNRS), Office of Research and Graduate Studies, and President's Office. Additionally we would like to thank Marty Reed in the CNRS machine shop for carefully fabricating custom items for our laboratory. Professor Wes Bliven contributed to the optical readout circuit design. Undergraduate students Noah Billings, Jacob Crummey, Holly Edmundson, Edward Kemper, Krystal Leigh-Logan, and Nathan Rasmussen have also contributed to this research.

8. References

1. N. Arkani-Hamed, S. Dimopoulos and G.R. Dvali, "New dimensions at a millimeter to a fermi and superstrings at a TeV," *Phys. Lett. B* **436**, 257 (1998).
2. D.B. Kaplan and M.B. Wise, "Couplings of a light dilaton and violations of the equivalence principle," *JHEP* **0008**, 037 (2000).
3. S. Perlmutter *et al.*, "Measurements of W and Λ from 42 high-redshift supernovae," *Astrophys. J.* **517**, 565 (1999).
4. C.D. Hoyle *et al.*, "Submillimeter tests of the gravitational inverse-square law," *Phys. Rev. D* **70**, 042004 (2004).
5. R. Sundrum, "Fat gravitons, the cosmological constant and submillimeter tests," *Phys. Rev. D* **69**, 044014 (2004).
6. D.J. Kapner *et al.*, "Tests of the gravitational inverse-square law below the dark-energy length scale," *Phys. Rev. Lett.* **98** 021101 (2007).
7. S.J. Smullin *et al.*, "Constraints on Yukawa-type deviations from Newtonian gravity at 20 microns," *Phys. Rev. D* **72**, 122001 (2005).
8. J.K. Hoskins *et al.*, "Experimental tests of the gravitational inverse-square law for mass separations from 2 to 105 cm," *Phys. Rev. D* **32**, 3084 (1985).
9. E.G. Adelberger, N.A. Collins, and C.D. Hoyle, "Analytic expressions for gravitational inner multipole moments of elementary solids and for the force between two rectangular solids," *Class. Quant. Grav.* **23** 125-136 (2006).